

Novel sodium aluminium borohydride containing the complex anion $[\text{Al}(\text{BH}_4,\text{Cl})_4]^-$

Inge Lindemann,^{*a} Roger Domènech Ferrer,^a Lothar Dunsch,^b Radovan Černý,^c Hans Hagemann,^d Vincenza D'Anna,^d Yaroslav Filinchuk,^e Ludwig Schultz^a and Oliver Gutfleisch^a

Received 16th December 2010, Accepted 7th February 2011

DOI: 10.1039/c0fd00024h

The synthesis of a novel alkali-metal aluminium borohydride $\text{NaAl}(\text{BH}_4)_x\text{Cl}_{4-x}$ from NaBH_4 and AlCl_3 using a solid state metathesis reaction is described. Structure determination was carried out using synchrotron powder diffraction data and vibrational spectroscopy. An orthorhombic structure (space group $Pmn2_1$) is formed which contains Na^+ cations and complex $[\text{Al}(\text{BH}_4,\text{Cl})_4]^-$ anions. Due to the high chlorine content ($1 \leq x \leq 1.43$) the hydrogen density of the borohydride is only between 2.3 and 3.5 wt.% H_2 in contrast to the expected 14.6 wt.% for chlorine free $\text{NaAl}(\text{BH}_4)_4$. The decomposition of $\text{NaAl}(\text{BH}_4)_x\text{Cl}_{4-x}$ is observed in the target range for desorption at about 90 °C by differential scanning calorimetry (DSC), *in situ* Raman spectroscopy and synchrotron powder X-ray diffraction. Thermogravimetric analysis (TG) shows extensive mass loss indicating the loss of H_2 and B_2H_6 at about 90 °C followed by extensive weight loss in the form of chloride evaporation.

1 Introduction

Borohydrides are of great research interest in the field of on-board hydrogen storage due to their high gravimetric and volumetric hydrogen density.¹ Many of these structures appear to be thermally very stable and consequently decompose at very high temperatures (*e.g.* LiBH_4 , $\text{Mg}(\text{BH}_4)_2$).^{2,3} The main focus in the search for new materials for hydrogen storage is to reduce their dehydrogenation temperature and to implement reversible hydrogen sorption reactions. The target temperature for desorption ideally matches the operating temperature of a PEM fuel cell which is between 60 and 120 °C.⁴ The desorption temperature of the borohydrides decreases with increasing Pauling electronegativity (χ_p) of the corresponding cation.⁵ Therefore partial substitution of the Na^+ cations ($\chi_p = 0.93$) with Al^{3+} cations ($\chi_p = 1.61$) in NaBH_4 may produce weakened B–H bonds.

There are a few reports on double-cation borohydrides $\text{A}_x\text{M}_y(\text{BH}_4)_z$ and the first theoretical and experimental studies point to an intermediate stability of the

^aFunctional Materials and Hydrides Group (Dept. 21), IFW Dresden, Helmholtzstrasse 20, D-01069 Dresden, Germany

^bDept. of Electrochemistry and Conducting Polymers, IFW Dresden, Helmholtzstrasse 20, D-01069 Dresden, Germany

^cLaboratory of Crystallography, University of Geneva, 24 quai Ernest-Ansermet, CH-1211 Geneva, Switzerland

^dDepartment of Physical Chemistry, University of Geneva, 30 quai Ernest-Ansermet, CH-1211 Geneva, Switzerland

^eInstitute of Condensed Matter and Nanosciences, Université Catholique de Louvain, Place L. Pasteur 1, B-1348 Louvain-la-Neuve, Belgium

corresponding single-cation borohydrides.^{6–8} Recently, LiK(BH₄)₂,⁸ LiSc(BH₄)₄⁹ and NaSc(BH₄)₄¹⁰ were synthesized. For applications in hydrogen storage their desorption temperatures are still too high with values of 380, 177 and 150 °C, respectively. A series of Zn-based mixed-metal borohydrides showed lower decomposition temperatures, ranging from 95 to 127 °C.¹¹ However these exhibit much lower hydrogen density. Al-Li-borohydride decomposes in the target range at about 70 °C, contains about 17.2 wt.% H₂ and shows a recently described distinctly novel structure.¹² The synthesis was carried out using mechano-chemical synthesis. This technique is widely used to prepare borohydrides by a metathesis reaction under moderate conditions.^{5,12,13} Another suitable candidate for lowering the dehydrogenation temperature is NaBH₄ which in turn is even more stable than LiBH₄. NaBH₄ is only desorbing at about 500 °C containing 10.8 wt.% H₂.¹⁴ Therefore a slightly higher decomposition temperature is expected for Na-Al-borohydride than the 70 °C of Al₃Li₄(BH₄)₁₃. The existence of [Al(BH₄)₄][−] anions was claimed in ref. 15 and confirmed in the structure of Al-Li-borohydride.¹² DFT calculations of various double-cation borohydrides by Hummelshøj *et al.*⁶ showed that NaAl(BH₄)₄ and LiAl(BH₄)₄ should be stable under ambient conditions. Al-Li-borohydride was already observed experimentally however it shows the different chemical formula Al₃Li₄(BH₄)₁₃.

Herein, we report on the synthesis and detailed structural, physical and chemical characterisation of a complex Na-Al-borohydride. The structure was determined by synchrotron powder diffraction experiments and further structural characterisation was done by vibrational spectroscopy (Raman and IR). To identify the modes observed in the Raman and IR spectra, a simulation for the anion [Al(BH₄,Cl)₄][−] was carried out in different compositions. The compound under study shows decomposition at moderate temperatures at about ~90 °C. However the practical hydrogen density (2.3–3.5 wt.% H₂) is much lower than the theoretical one (14.6 wt.%) because of the very high amount of chlorine in the structure. A quite high amount of AlCl₃ is needed to form high weight fractions of the new phase. Therefore it contains a lot of chlorine which is incorporated into the structure instead of (BH₄)[−].

2 Experimental

2.1 Structural characterisation

AlCl₃ (Merck, purity 98 wt.%) and NaBH₄ (Sigma-Aldrich, purity 99 wt.%) mixed in different molar ratios (1 : 1, 1 : 2, 1 : 3 and 1 : 4) were ball milled for 5 h under argon atmosphere (Fritsch P6, 500 rpm) with a ball to powder ratio of 40 : 1. Sample preparation and handling was always carried out in an argon filled glovebox with an oxygen and water content less than 2 ppm. During the milling process, the pressure and temperature were continuously *in situ* monitored to follow any hydrogen evolution processes (Evico Magnetics device).^{16,17} Transmission X-ray diffraction measurements were performed in glass capillaries (outer diameter 0.7 mm) on a Stoe Stadi P (Mo K_{α1}) in Debye–Scherrer geometry in the range of 3° ≤ 2θ ≤ 35° with a step size of 0.02° 2θ at room temperature. The diffractometer is equipped with a curved Ge(111) monochromator and a 6°-linear position sensitive detector with a resolution of about 0.06° 2θ at full width-half maximum (FWHM).

Synchrotron radiation *in situ* powder X-ray diffraction (SR-PXD) data of the 1 : 1 and 1 : 2 powders was collected at the SNBL (Grenoble, France) with a MAR345 detector and the selected X-ray wavelength of 0.7004 Å. The temperature dependent data between 173 and 227 °C (Oxford Cryostream 700+) has been measured for the 1 : 1 mixture. The 1 : 3 powder was measured at the SLS (PSI Villigen, Switzerland, λ = 0.7296 Å, Mythen detector) and the temperature dependent data (Stoe capillary furnace) has been measured between 30 and 200 °C. The

1 : 4 mixture has been measured at the SNBL ($\lambda = 0.7296 \text{ \AA}$, multi-crystal analyzer). All samples were filled in a glass capillary with an outer diameter of 0.8 mm. All 2D SR-PXD data were integrated into 1D patterns using the Fit2D program.¹⁸ The SLS data which has simultaneously high angular resolution and excellent statistics of counts has been used for indexing, structure solution and final Rietveld refinement. Beside the peaks of NaBH₄ and NaCl, strong peaks belonging to an unknown phase were observed which disappear simultaneously at $\sim 87^\circ\text{C}$. The first 20 peaks of the new phase were indexed by using Dicvol04¹⁹ in an orthorhombic cell indicating clearly the space group *Pmn2*₁ (see Table 2). The structure has been solved with the direct space method program FOX,²⁰ and refined with the Rietveld method using the TOPAS program.²¹ The symmetry of the refined structure has been checked with the routine ADDSYM in the program PLATON,²² and the space group *Pmn2*₁ has been confirmed. The resulting structure containing one Na atom (position 2*a*), one Al atom (position 2*a*), 2 BH₄ groups (position 2*a*) and one Cl atom (4*b*) in the asymmetric unit, was refined by the Rietveld method. The refinement suggests partial substitution of BH₄ groups by Cl atoms (see Table 2). The structure was solved and refined with the BH₄ groups as semi-rigid ideal tetrahedra with one common refined B–H distance. For two boron atoms situated on the mirror plane symmetry the BH₄ tetrahedra were allowed only to translate and to rotate following the mirror plane symmetry. Four anti-bump distance restraints were needed to stabilize the shape and orientation of the complex anion [Al(BH₄,Cl)₄]⁻ in the structure: Al–H 1.7, Al–Cl 2.1, Al–B 2.2 and Na–H 2.3 \AA . The individual displacement parameters for each atom type have been refined isotropically. The uncertainties of crystallographic coordinates of hydrogen atoms were not available from the least squares matrix, and were estimated by the bootstrap method.²³ The final refinement suggests also partial substitution of BH₄ groups by Cl atoms (and *vice versa*) in NaBH₄ and NaCl (for substitution rates see Table 1), and traces of NaAlCl₄. The agreement factors are: R_{wp} (not corrected for background) = 4.58%, R_{wp} (corrected for background) = 10.76%, $\chi^2 = 12.11$, R_{Bragg} (NaAl(BH₄,Cl)₄) = 1.75%. The high value of χ^2 reflects mainly the extremely high counting statistics of the powder diffraction data obtained from modern X-ray detectors.

Raman measurements were performed with an Ar⁺ laser (Innova 305 Coherent) with a wavelength of $\lambda = 514 \text{ nm}$. The spectra were recorded by a T-64000 spectrometer (Horiba) with a spectral resolution of 1 cm^{-1} . The spectrometer was calibrated before each series of measurements by using the F_{1g} mode of Si at 520.2 cm^{-1} . IR spectra were obtained at room temperature using a Biorad Excalibur FT-IR instrument with a nominal resolution of 1 cm^{-1} . Structural optimization of the [Al(BH₄)_xCl_{4-x}]⁻ ion and frequency calculation for its IR and Raman spectra were carried out using TURBOMOLE package. For all the atoms TZVP basis sets were used and the chosen functional was B3-LYP. The optimization with the B3-LYP Gaussian functional was not able to calculate the frequencies because the frequency calculations are not implemented for this functional. The charge –1 and singlet spin state was assumed.

Composition analysis of the evaporation product of the 1 : 1 powder was carried out using the EDX detector in a scanning electron microscope (SEM) (Leo 1530 Gemini).

2.2 Thermal characterisation

Thermodynamic characterization was performed by DSC (Seteram, Sensys evo) and TG (IGA Hiden Isochema) in 1 bar Ar with a constant heating rate of 5 K min⁻¹. *In situ* Raman measurements were carried under the same conditions as mentioned above in a dedicated pressure cell designed for temperature and pressure dependent studies.²⁴ The measurements were carried out in Ar atmosphere up to 250 °C.

3 Results and discussion

3.1 Structural characterisation

High-energy ball milling was used for the metathesis reaction between AlCl_3 and NaBH_4 . During the milling process no pressure increase was observed which indicates that no starting material is evaporated by the milling process and no hydrogen is desorbed. Structural analysis by transmission XRD (see Fig. 1) shows several unknown peaks at low angles (*) which point to the formation of a new phase with rather a large unit cell. These were further analysed using synchrotron radiation X-ray powder diffraction. In most of the samples solid solutions of $\text{Na}(\text{BH}_4,\text{Cl})$ are observed as impurities, mostly as two phases, a borohydride rich $\text{Na}(\text{BH}_4)_x\text{Cl}_{1-x}$ and a chlorine rich $\text{NaCl}_x(\text{BH}_4)_{1-x}$ phase, showing the limited solubility of NaBH_4 and NaCl . With increasing ratio of NaBH_4 the fraction of $\text{Na}(\text{BH}_4)_x\text{Cl}_{1-x}$ also increases. This is observed with shifted positions in comparison to pure NaBH_4 due to chlorine incorporation. The radius of the chlorine ion is only 1.68 Å in contrast to 2.05 Å for the $[\text{BH}_4]^-$ ion which results in a smaller lattice parameter for $\text{Na}(\text{BH}_4)_x\text{Cl}_{1-x}$ as shown in Table 1.

The main phase in the 1 : 1 mixture (AlCl_3 : NaBH_4) is the new alkali-metal aluminium-borohydride $\text{NaAl}(\text{BH}_4)_x\text{Cl}_{4-x}$. In the molar ratio 1 : 1 the ternary chloride NaAlCl_4 is formed instead of $\text{Na}(\text{BH}_4)_x\text{Cl}_{1-x}$. All powders (1 : 1, 1 : 2, 1 : 3 and 1 : 4, AlCl_3 : NaBH_4) contain the novel alkali-metal aluminium-borohydride $\text{NaAl}(\text{BH}_4)_x\text{Cl}_{4-x}$. With increasing amount of NaBH_4 its weight fraction is reduced. Therefore the highest yield of $\text{NaAl}(\text{BH}_4)_x\text{Cl}_{4-x}$ is present in the 1 : 1 mixture, however this also shows the highest chlorine content. $\text{NaAl}(\text{BH}_4)_x\text{Cl}_{4-x}$ crystallizes in the orthorhombic space group $Pmn2_1$ and contains the tetrahedral complex anion $[\text{Al}(\text{BH}_4)_x\text{Cl}_{4-x}]^-$. It is formed only in a quite narrow range of compositions with minimum 25 mol% ($x = 1$) as observed in the 1 : 1 powder, and with maximum 36 mol% ($x = 1.43$) of $[\text{BH}_4]^-$ in the 1 : 3 powder. The borohydride ion prefers two atomic sites with higher local symmetry on the mirror plane (see Fig. 2). The third atomic site, the general position, is exclusively occupied by Cl^- ions. The refined composition of mixed phases, their lattice dimensions and weight fractions in the samples at room temperature are given in Table 1.

The structural data of $\text{NaAl}(\text{BH}_4)_x\text{Cl}_{4-x}$ refined from the room temperature powder pattern of the 1 : 3 mixture are given in Table 2. The lattice parameters are $a = 7.90005(39)$, $b = 7.00328(32)$ and $c = 6.48883(26)$ Å. The occupancy of

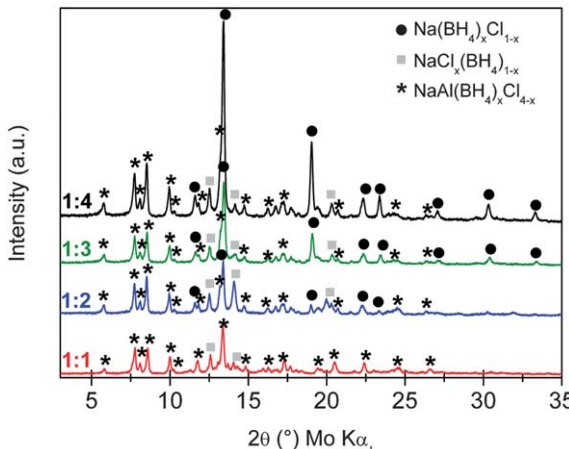
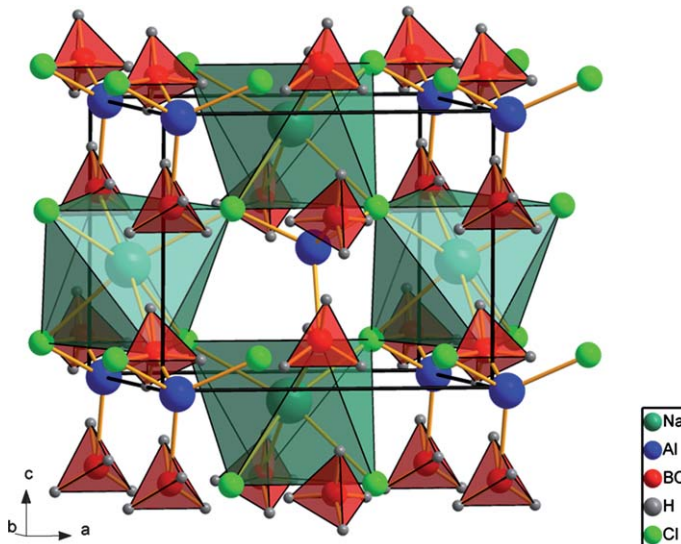


Fig. 1 XRD patterns of the 1 : 1 (red), 1 : 2 (blue), 1 : 3 (green) and 1 : 4 (black) molar ratio powder (AlCl_3 : NaBH_4).

Table 1 Refined composition of mixed phases, their lattice dimensions and weight fractions in the 1 : 1, 1 : 2, 1 : 3 and 1 : 4 mixture ($\text{AlCl}_3\text{:NaBH}_4$) at room temperature

	$\text{NaAl}(\text{BH}_4)_x\text{Cl}_{4-x}$			$\text{Na}(\text{BH}_4)_x\text{Cl}_{1-x}$			$\text{NaCl}_x(\text{BH}_4)_{1-x}$			NaAlCl_4	
	x	V ³	wt.%	x	a	wt. %	x	a	wt. %	wt. %	
1 : 1	1.00(4)	351.1(1)	78(1)	—	—	—	1	5.677(1)	1.0(2)	21(1)	
2 : 1	1.40(4)	358.8(1)	69(1)	0.86(3)	6.067(1)	12(1)	0.76(5)	5.7780(8)	19(1)	—	
3 : 1	1.43(4)	359.00(3)	49.9(4)	0.799(4)	6.0517(1)	45.5(4)	0.86(7)	5.801(2)	3.4(3)	1.2(2)	
4 : 1	1.40(4)	358.58(2)	48.5(3)	0.795(5)	6.0597(1)	51.5(3)	—	—	—	—	

**Fig. 2** Unit cell of $\text{NaAl}(\text{BH}_4)_x\text{Cl}_{4-x}$ containing the new complex anions $[\text{Al}(\text{BH}_4)_x\text{Cl}_{4-x}]^-$ with the Na^+ counter cations.

site B1 is 0.82(2) by $[\text{BH}_4]^-$ and 0.18(2) by Cl^- and of site B2 it is 0.609(7) by $[\text{BH}_4]^-$ and 0.391(2) by Cl^- . The z-coordinate of Al was fixed to 0.5 during the refinement (polar space group). The unit cell is shown in Fig. 2 whereas complex anions $[\text{Al}(\text{BH}_4)_x\text{Cl}_{4-x}]^-$ are counteracting with Na^+ cations.

The crystal structure of $\text{NaAl}(\text{BH}_4)_x\text{Cl}_{4-x}$ can be compared with that of the alkaline aluminium chlorides. The latest structural data of NaAlCl_4 were published by Krebs *et al.*²⁵ A review of different structures of $A\text{AlCl}_4$ ($A = \text{Li}, \text{Na}, \text{K}, \text{Rb}, \text{Cs}$) shows that in all structures there is an $[\text{AlCl}_4]^-$ anion with Al–Cl distance within 2.111–2.268 Å.²⁶ The comparison of the coordination of the alkaline metal with Cl^- or $[\text{BH}_4]^-$ and the alkaline metal with aluminium is given in Table 3. It shows that Na^+ changes the coordination in both cases to the one of smaller Li^+ when partly replacing Cl^- by $[\text{BH}_4]^-$ in the complex anion $[\text{AlCl}_4]^-$. It is certainly a size effect as $[\text{Al}(\text{BH}_4,\text{Cl})_4]^-$ is bigger than $[\text{AlCl}_4]^-$. However, the connectivity is different in LiAlCl_4 and in $\text{NaAl}(\text{BH}_4)_x\text{Cl}_{4-x}$ certainly due to the electronic effect, as the directional bonding of the $[\text{BH}_4]^-$ and Cl^- ligands is not the same. Contrary to Sc based compounds like $\text{LiSc}(\text{BH}_4)_4$,⁹ $\text{NaSc}(\text{BH}_4)_4$ ¹⁰ and $\text{KSc}(\text{BH}_4)_4$ ²⁷ containing the complex anion $[\text{Sc}(\text{BH}_4)_4]^-$, the complex anion $[\text{Al}(\text{BH}_4)_4]^-$ is difficult to stabilize, probably because Al^{3+} is too small compared to Sc^{3+} . The anion can be stabilized by partial substitution of its $[\text{BH}_4]^-$ ligands by smaller Cl^- , or by making its

Table 2 Atomic coordinates of $\text{NaAl}(\text{BH}_4)_x\text{Cl}_{4-x}$, space group $Pmn2_1$, $a = 7.90005(39)$, $b = 7.00328(32)$, $c = 6.48883(26)$ Å, $V = 359.003(28)$ Å³ at room temperature. Mixture 3 : 1^a

Atom	Site	<i>x</i>	<i>y</i>	<i>Z</i>	$B_{\text{iso}}/\text{\AA}^2$
Na	2a	1/2	0.5387(5)	0.9094(7)	4.0(3)
Al	2a	1/2	0.1916(4)	0.5	4.0(3)
B1	2a	1/2	0.8839(1)	0.5589(1)	2.0(9)
H11	2a	1/2	0.7685(1)	0.4366(1)	2.5(9)
H12	2a	1/2	0.8156(1)	0.7171(1)	$= B_{\text{iso}}(\text{H11})$
H13	4b	0.3829(1)	0.9758(1)	0.5409(1)	$= B_{\text{iso}}(\text{H11})$
B2	2a	1/2	0.1274(1)	0.1315(1)	$= B_{\text{iso}}(\text{B1})$
H21	2a	1/2	0.0461(1)	0.2824(1)	$= B_{\text{iso}}(\text{H11})$
H22	2a	1/2	0.2863(1)	0.1640(1)	$= B_{\text{iso}}(\text{H11})$
H23	4b	0.3829(1)	0.0886(1)	0.0399(1)	$= B_{\text{iso}}(\text{H11})$
Cl3	4b	0.2120(3)	0.6676(4)	0.1220(7)	4.0(1)

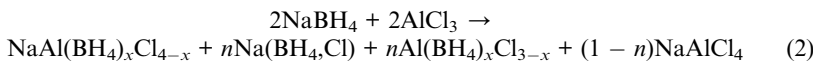
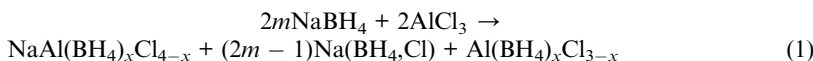
^a Occupancy of site B1: BH₄ 0.82(2), Cl 0.18(2). Occupancy of site B2: BH₄ 0.609(7), Cl 0.391(2). *z*-coordinate of Al fixed to 0.5 (polar space group).

Table 3 Coordination of alkaline metal with Cl⁻ or [BH₄]⁻ and with aluminium for LiAlCl₄, NaAlCl₄ and NaAl(BH₄)_xCl_{4-x}

	LiAlCl ₄	NaAlCl ₄	NaAl(BH ₄) _x Cl _{4-x}
CN <i>A</i> -Cl, BH ₄	6 (octahedron)	8 (bicapped trigonal prism)	6 (octahedron)
CN <i>A</i> -Al	4 (tetrahedron)	6 (trigonal prism)	4 (tetrahedron)

[BH₄]⁻ ligands bridging rather than terminal, as in the Li containing compound Al₃Li₄(BH₄)₁₃.¹²

The powder patterns of the 1 : 1, 1 : 2 and 1 : 3 mixtures also showed additional peaks which are not fully understood yet. There is an unknown phase (phase no. 2 in Fig. 8) and a phase which has been tentatively associated to Al(BH₄)_xCl_{3-x} (phase no. 1 in Fig. 8) from the agreement of positions of some peaks with β-Al(BH₄)₃.²⁸ However, the peaks are too weak for any structural solution. We can only speculate that it is possible to stabilise solid β-Al(BH₄)₃ by chlorine incorporation as it is liquid at room temperature, and it would be decomposed during the milling process since its decomposition is already occurring at about 50 °C.⁴ Furthermore the reaction pathway seems to be different for the 1 : 1 molar ratio than for the other mixtures where an excess of NaBH₄ is used. For mixtures with an excess of NaBH₄ reaction (1) might be occurring. The equal molar ratio 1 : 1 directly forms the ternary chloride NaAlCl₄ as shown in reaction (2).



For further structural characterisation vibrational spectroscopy was carried out. The IR (a) and Raman (b) spectra of the different powders are shown in Fig. 3. In agreement with XRD measurements all powders except that of the 1 : 1 ratio show extensive modes of NaBH₄ (IR: bending 1119 cm⁻¹, stretching 2300 cm⁻¹; Raman: bending 1285 cm⁻¹, stretching 2345 cm⁻¹).²⁹ The corresponding intensities

increase with increasing excess of NaBH_4 (lower molar ratio of $\text{AlCl}_3 : \text{NaBH}_4$). All spectra show a mode at 490 cm^{-1} as observed in Al-Li-borohydride corresponding to the mode from Al-B.¹² Unknown modes in the $[\text{BH}_4]^-$ stretching range correspond to the vibrations of $[\text{Al}(\text{BH}_4)_x\text{Cl}_{4-x}]^-$ present in both the new alkali-metal aluminium borohydride $\text{NaAl}(\text{BH}_4)_x\text{Cl}_{4-x}$ as well as the chlorine stabilised aluminium borohydride $\text{Al}(\text{BH}_4)_x\text{Cl}_{3-x}$ (IR: 2160 cm^{-1} , 2444 cm^{-1} , 2503 cm^{-1} ; Raman: 2180 cm^{-1} , 2455 cm^{-1} , 2510 cm^{-1}). This was confirmed by simulations of the IR (a) and Raman (b) spectra of the anion containing various chlorine contents ($x = 1, 2, 3, 4$) which are shown in Fig. 4. It is not possible to determine the exact chlorine content from the IR and Raman spectra. Nevertheless, the theoretical IR and Raman spectra for $[\text{Al}(\text{BH}_4)_2\text{Cl}_2]^-$ and $[\text{Al}(\text{BH}_4)\text{Cl}_3]^-$ are in good agreement with the spectra of the 1 : 1 powder where the fraction of the new phase is the highest (see Fig. 4). We observe a bidendate binding whereas 2160 cm^{-1} indicates the stretching mode of the inner hydrogen atoms and at 2444 cm^{-1} and 2503 cm^{-1} the stretching modes of the outer atoms are observed. The Raman spectra show one of the four fundamental modes of $[\text{AlCl}_4]^-$ at $\nu_1 (\text{A}_1) = 349\text{ cm}^{-1}$ as found in NaAlCl_4 .^{30,31} The sharp bands around 400 cm^{-1} are related to Al-Cl modes in $\text{Al}(\text{BH}_4)_x\text{Cl}_{3-x}$ and $[\text{Al}(\text{BH}_4)_x\text{Cl}_{4-x}]^-$. The broad peak at about 490 cm^{-1} can be associated with the mode of Al-B as also found in Al-Li-borohydride with respect to the pure $\text{Al}(\text{BH}_4)_3$.¹² The vibration at 350 cm^{-1} increases steadily with higher molar ratio. This fits very well with the observation of the ternary NaAlCl_4 in the 1 : 1 mixture.

Furthermore the peak position of the frequency ν_3 in $\text{Na}(\text{BH}_4,\text{Cl})_4$ changes with respect to the chlorine content. In Fig. 5 this peak position in the IR spectra is shown for various chlorine contents in the different samples. With increasing chlorine content the frequency is smaller which might be due to the heavier Cl^- ion.

3.2 Thermal characterisation

The thermal behaviour of the different mixtures (1 : 1, 1 : 2, 1 : 3, 1 : 4 of $\text{AlCl}_3 : \text{NaBH}_4$) was analysed by differential scanning calorimetry (DSC), thermo-gravimetry (TG) and *in situ* techniques of Raman spectroscopy and synchrotron radiation X-ray diffraction. Fig. 6(a) shows the DSC measurements of the four different mixtures in 1 bar Ar atmosphere. All different molar ratios show two endothermic peaks superimposed on each other with an onset at about 90°C . This might be attributed to the simultaneous decomposition of $\text{NaAl}(\text{BH}_4)_x\text{Cl}_{4-x}$ and $\text{Al}(\text{BH}_4)_x\text{Cl}_{3-x}$. As expected from the weight fractions of the new alkali-metal aluminium borohydride the enthalpy decreases with increasing excess of NaBH_4 . The 1 : 1 molar ratio ($\text{AlCl}_3 : \text{NaBH}_4$) powder shows the highest heat of decomposition (67.2 J g^{-1}) due to the highest fraction of $\text{NaAl}(\text{BH}_4)_x\text{Cl}_{4-x}$ (78.0 wt.%) in the powder. The 1 : 2 and 1 : 3 molar ratio powders show lower values of 51.9 J g^{-1} (69.0 wt.%) and

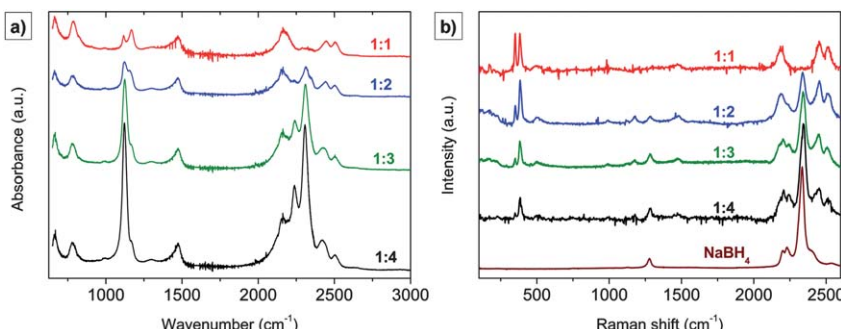


Fig. 3 a) IR and b) Raman spectra of the different molar ratios ($\text{AlCl}_3 : \text{NaBH}_4$) in red (1 : 1), blue (1 : 2), green (1 : 3) and black (1 : 4).

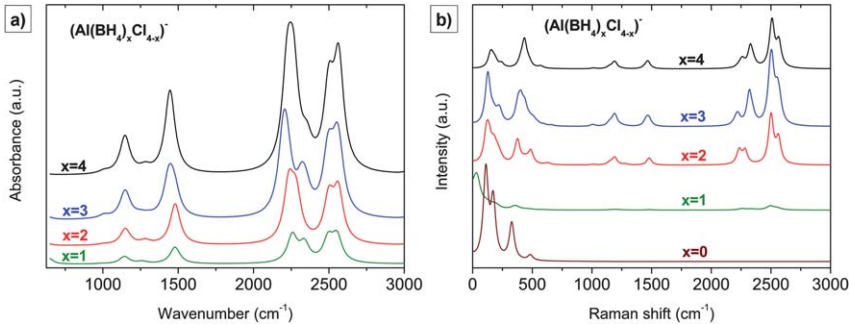


Fig. 4 Simulated a) IR and b) Raman spectra of $[\text{Al}(\text{BH}_4)_x\text{Cl}_{4-x}]^-$ for $x = 4$ (black), $x = 3$ (blue), $x = 2$ (red), $x = 1$ (green).

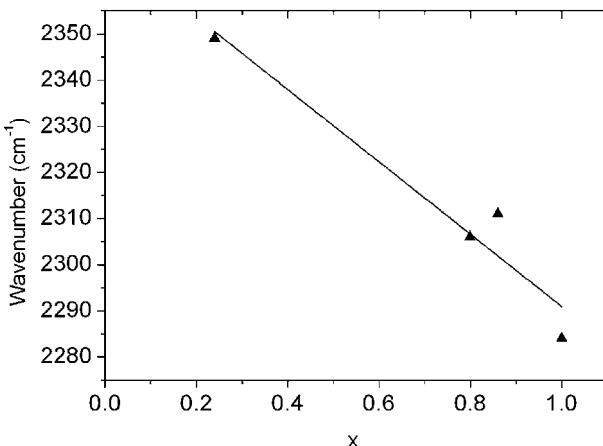


Fig. 5 Peak position of ν_3 in the IR spectrum of $\text{Na}(\text{BH}_4)_{1-x}\text{Cl}_x$ vs. refined composition.

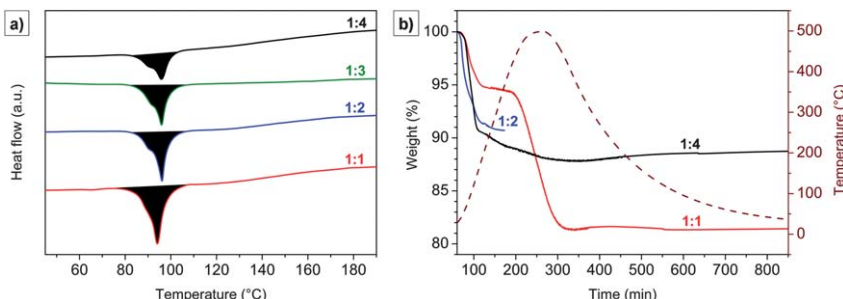


Fig. 6 a) DSC measurements of powders in the 1 : 1, 1 : 2, 1 : 3 and 1 : 4 molar ratios ($\text{AlCl}_3 : \text{NaBH}_4$) in 1 bar Ar up to 300 °C with 5 K min⁻¹ heating rate and b) TG measurements vs. time of the 1 : 1, 1 : 2 and 1 : 4 molar ratios in 1 bar Ar with 5 K min⁻¹ heating rate (temperature profile plotted with the dashed line).

46.5 J g⁻¹ (49.9 wt.%), respectively, due to the reduced fraction of $\text{NaAl}(\text{BH}_4)_x\text{Cl}_{4-x}$. For the 1 : 4 molar ratio the lowest heat of decomposition is observed (32.2 J g⁻¹), although it contains nearly the same amount of $\text{NaAl}(\text{BH}_4)_x\text{Cl}_{4-x}$ (48.5 wt.%) as the 1 : 3 powder (49.9 wt.%). Nevertheless, it was mentioned before that the 1 : 4

mixture did not show unknown phases as $\text{Al}(\text{BH}_4)_x\text{Cl}_{3-x}$. Therefore the enthalpy is much lower than in the 1 : 3 mixture.

Furthermore, at least for the 1 : 1 molar ratio powder an additional endothermic peak at about 150 °C was expected since the melting of the ternary chloride NaAlCl_4 occurs at this temperature.²⁵ This is actually not observed in any of the DSC measurements which could be explained by incongruent melting of this phase. Due to the high volatility of AlCl_3 , an equimolar melt is seldom possible. Therefore solid NaAlCl_4 melts incongruently with a composition deficient in AlCl_3 .³²

Fig. 6(b) shows the thermogravimetric (TG) measurements of the 1 : 1 and 1 : 4 powders up to 500 °C. The 1 : 2 powder was only measured up to 150 °C due to the strong evaporation starting at about 150 °C. This contaminates the thermocouple of the device and should be avoided if possible. The strong evaporation was also observed by *in situ* Raman spectroscopy in the 1 : 2, 1 : 3 and 1 : 4 powders. The 1 : 1 powder shows only a weak evaporation around this temperature but an even stronger one between 250 and 400 °C. The weight loss above 150 °C is most probably due to the evaporation of AlCl_3 and Na. All powders show an extensive mass loss at about 90 °C where the decomposition of $\text{NaAl}(\text{BH}_4)_x\text{Cl}_{4-x}$ and $\text{Al}(\text{BH}_4)_x\text{Cl}_{3-x}$ was observed by DSC analysis. Assuming that all $[\text{BH}_4]^-$ groups of $\text{NaAl}(\text{BH}_4)_x\text{Cl}_{4-x}$ are lost after decomposition in the form of H_2 and B_2H_6 , in the 1 : 2 molar ratio powder a weight loss of about 8.8 wt.% is expected and we do observe 9.4 wt.%. Therefore Na or some chlorine species has already started to evaporate. The 1 : 4 powder shows experimentally an even higher weight loss of about 11.2 wt.% which also points to the loss of Na and chlorine species. Surprisingly, a two step weight loss behaviour is observed for the 1 : 1 molar ratio powder. The yield of $\text{NaAl}(\text{BH}_4)_x\text{Cl}_{4-x}$ is the highest with 78 wt.%. However, in the 1 : 1 powder the chlorine content is higher ($x = 1.00$, 75 mol%) than in the 1 : 2 ($x = 1.40$, 65 mol%) powder and therefore the mass loss around 90 °C should be higher in the 1 : 2 powder as observed. The loss based on H_2 and B_2H_6 is theoretically 6.7 wt.% and we observe 5.5 wt.%. The total mass loss after the 2nd step is about 18.5 wt.% and can be associated with the strong evaporation losing Na and AlCl_3 . The evaporation of Na, Al and Cl in this 1 : 1 molar ratio was confirmed by SEM-EDX measurements. In Table 4 the theoretically expected weight loss during decomposition of $\text{NaAl}(\text{BH}_4)_x\text{Cl}_{4-x}$ is shown for the different mixtures when losing only $[\text{BH}_4]^-$ groups. The observed weight loss is always higher than the theoretical one due to the volatility of $\text{Al}(\text{BH}_4)_x\text{Cl}_{3-x}$ and the evaporation of Na and chlorine species.

In situ spectroscopic analysis should give more information about the decomposition pathway of the compound. *In situ* Raman analysis of the 1 : 1 (a) and the 1 : 3 powder (b) is shown in Fig. 7. Both spectra at room temperature show the pattern of the new alkali-metal aluminium borohydride decomposing above 70 °C which is in good agreement with DSC measurements where the decomposition was observed at about 90 °C. During decomposition the mode at 380 cm⁻¹ firstly increases, which means the increase of the Al–Cl mode, and then disappears in

Table 4 Theoretical weight loss for the 1 : 1, 1 : 2, 1 : 3 and 1 : 4 mixtures assuming only the loss of $(\text{BH}_4)^-$ from $\text{NaAl}(\text{BH}_4)_x\text{Cl}_{4-x}$

Mixture	Chlorine content	Molar mass $\text{NaAl}(\text{BH}_4)_x\text{Cl}_{4-x}/\text{g mol}^{-1}$	Wt.% of $\text{NaAl}(\text{BH}_4)_x\text{Cl}_{4-x}$	Weight loss by loss of $[\text{BH}_4]^-/\text{wt.}\%$
1 : 1	$x = 1.00$	171.2	78.0	6.7
1 : 2	$x = 1.40$	162.9	69.0	8.8
1 : 3	$x = 1.43$	162.2	49.9	6.5
1 : 4	$x = 1.40$	162.9	48.5	6.2

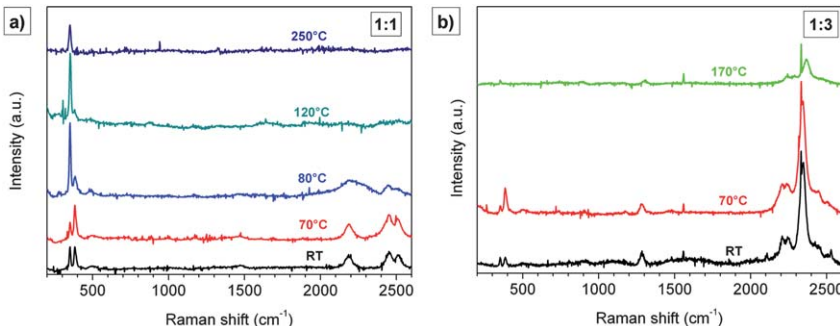


Fig. 7 Temperature dependent *in situ* Raman measurements of a) the 1 : 1 and b) the 1 : 3 powder in Ar atmosphere from room temperature (RT) up to 250 and 170 °C, respectively.

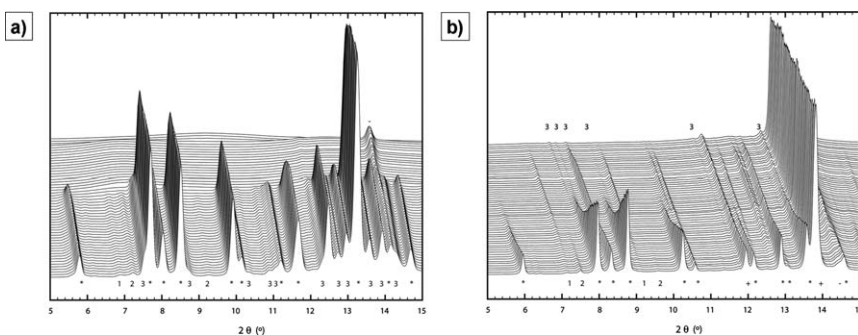


Fig. 8 *T*-ramp from the SR-PXD of a) the 1 : 1 mixture from 20 to 125 °C ($\lambda = 0.7004 \text{ \AA}$) and of b) the 1 : 3 mixture from 62 to 125 °C ($\lambda = 0.7296 \text{ \AA}$). Symbols: * $\text{NaAl}(\text{BH}_4)_x\text{Cl}_{4-x}$, - $\text{NaCl}_x(\text{BH}_4)_{1-x}$, + $\text{Na}(\text{BH}_4)_x\text{Cl}_{1-x}$, 1 – possibly $\text{Al}(\text{BH}_4)_x\text{Cl}_{3-x}$, 2 – unknown phase, 3 – NaAlCl_4 .

both powders due to evaporation. In the 1 : 1 molar ratio only the mode corresponding to NaAlCl_4^{31} at 350 cm^{-1} is present at 250 °C and no traces of $\text{Na}(\text{BH}_4)_x\text{Cl}_{1-x}$ can be observed. In the 1 : 3 molar ratio the modes corresponding to $\text{Na}(\text{BH}_4)_x\text{Cl}_{1-x}$ can be observed at 2370 cm^{-1} and a tiny mode at 380 cm^{-1} can be observed which refers to NaAlCl_4 .

For comparison in Fig. 8 the *in situ* synchrotron analysis of the 1 : 1 (a) and the 1 : 3 mixture (b) is shown. In both measurements decomposition of $\text{NaAl}(\text{BH}_4)_x\text{Cl}_{4-x}$ can be observed since the corresponding peaks (*) are disappearing while heating at around 90 °C. The SR-PXD pattern of the phase formed after decomposition in the 1 : 1 mixture cannot be explained by this data. Nevertheless in the 1 : 3 mixture NaAlCl_4 is clearly formed after decomposition. The exact reaction pathway during composition is hard to assume due to strongly reactive species and very volatile materials.

4 Conclusion

A novel alkali-metal aluminium borohydride was synthesised by metathesis reaction of AlCl_3 and NaBH_4 carried out by ball milling in Ar atmosphere. The structure of the new phase was determined from SR-PXD measurements. $\text{NaAl}(\text{BH}_4)_x\text{Cl}_{4-x}$ forms an orthorhombic structure containing $(\text{Al}(\text{BH}_4)_x\text{Cl}_{4-x})^-$ anions and Na^+ counter cations. The new phase only forms in the quite narrow range of composition between $x = 1$ (25 mol% $[\text{BH}_4^-]$) and $x = 1.43$ (36 mol% $[\text{BH}_4^-]$). The high chlorine

content reduces the H₂ density extensively from theoretically 14.6 wt.% for NaAl(BH₄)₄ down to the range between 2.4 wt.% H₂ ($x = 1$) and 3.5 wt.% H₂ ($x = 1.43$) for the observed NaAl(BH₄)_xCl_{4-x}. The [Al(BH₄)_xCl_{4-x}]⁻ anion in the structure was confirmed by IR and Raman simulation which was done for different compositions ($x = 1, 2, 3, 4$). *In situ* Raman spectroscopy and *in situ* synchrotron data revealed more insight into the decomposition pathway of the compound and confirmed the decomposition at around 90 °C as observed by DSC and TG. An extensive weight loss was observed during decomposition which is due to the loss of not only H₂ but also B₂H₆, chlorine and other reactive species. The weight fraction of the alkali-metal aluminium borohydride is highest in the 1 : 1 molar ratio mixture, however the chlorine content is also the highest in this mixture. It appears that the compound can only be stable with incorporated chlorine in contrast to the theoretically predicted stability of pure NaAl(BH₄)₄. Nevertheless, the stability of the chloridic sodium aluminium borohydride is slightly higher (~90 °C) than the one observed for Al-Li-borohydride (~70 °C), as expected. Its stability is higher than that for pure Al(BH₄)₃ due to the Cl⁻ substitution and the addition of Na⁺ cations. Due to the extensive loss of chlorine species and the highly reactive decomposition products it is not possible to recharge the powders. Therefore an attempt for pure preparation of chlorine free NaAl(BH₄)₄ will be made although it is likely to be unstable.

Acknowledgements

Authors are grateful to the European Union as well as the Free State of Saxony (ECEMP 13853/2379) and for technical assistance by Monika Herrich and Bernhard Gebel. This work was supported by the Swiss National Science Foundation. The authors acknowledge SNBL and SLS for the beam time allocation.

References

- 1 S. Orimo, Y. Nakamori, J. R. Eliseo, A. Züttel and C. M. Jensen, *Chem. Rev.*, 2007, **107**, 4111.
- 2 M. D. Riktor, M. H. Sorby, K. Chlopek, M. Fichtner, F. Buchter, A. Züttel and B. C. Hauback, *J. Mater. Chem.*, 2007, **17**, 4939–4942.
- 3 U. Bösenberg, *et al.*, *Acta Mater.*, 2007, **55**, 3951–3958.
- 4 W. Gochala and P. P. Edwards, *Chem. Rev.*, 2004, **104**, 1283–1315.
- 5 Y. Nakamori, K. Miwa, A. Ninomiya, H. Li, N. Ohba, S. Towata, A. Züttel and S. Orimo, *Phys. Rev. B: Condens. Matter Mater. Phys.*, 2006, **74**, 045126.
- 6 J. S. Hummelsøj, D. D. Landis, J. Voss, T. Jiang, A. Tekin, N. Bork, M. Dulak, J. J. Mortensen, L. Adamska and J. Andersin, *J. Chem. Phys.*, 2009, **131**, 014101.
- 7 X.-B. Xiao, W.-Y. Yu and B.-Y. Tang, *J. Phys.: Condens. Matter*, 2008, **20**, 445210.
- 8 E. A. Nickels, M. O. Jones, W. I. F. David, S. R. Johnson, R. L. Lowton, M. Sommariva and P. P. Edwards, *Angew. Chem., Int. Ed.*, 2008, **47**, 2817–2819.
- 9 H. Hagemann, M. Longhini, J. W. Kaminski, T. A. Wesolowski, R. Černý, N. Penin, M. Sørby, B. Hauback, G. Severa and C. Jensen, *J. Phys. Chem. A*, 2008, **112**, 7551–7555.
- 10 R. Černý, G. Severa, D. Ravnsbæk, Y. Filinchuk, V. d'Anna, H. Hagemann, D. Haase, C. M. Jensen and T. R. Jensen, *J. Phys. Chem. C*, 2010, **114**, 1357–1364.
- 11 D. Ravnsbæk, Y. Filinchuk, Y. Cerenius, H. J. Jakobsen, F. Besenbacher, J. Skibsted and T. R. Jensen, *Angew. Chem., Int. Ed.*, 2009, **48**, 6659–6663.
- 12 I. Lindemann, R. Domènech Ferrer, L. Dunsch, Y. Filinchuk, R. Černý, H. Hagemann, V. D'Anna, L. M. Lawson Daku, L. Schultz and O. Gutfleisch, *Chem.-Eur. J.*, 2010, **16**, 8707–8712.
- 13 C. Rongeat, I. Lindemann, A. Borgschulte, L. Schultz and O. Gutfleisch, *Int. J. Hydrogen Energy*, 2011, **36**, 247–253.
- 14 J. Urgnani, F. J. Torres, M. Palumbo and M. Baricco, *Int. J. Hydrogen Energy*, 2008, **33**, 3111–3115.
- 15 L. V. Titov and E. R. Eremin, *Bull. Acad. Sci. USSR, Div. Chem. Sci. (Engl. Transl.)*, 1975, **24**, 1095.
- 16 C. Rongeat, I. Llamas-Jansa, S. Doppiu, S. Deledda, A. Borgschulte, L. Schultz and O. Gutfleisch, *J. Phys. Chem. B*, 2007, **111**, 13301.

- 17 C. Rongeåt, I. L. Jansa, S. Oswald, L. Schultz and O. Gutfleisch, *Acta Mater.*, 2009, **57**, 5563–5570.
- 18 A. P. Hammersley, S. O. Svensson, M. Hanfland, A. N. Fitch and D. Häusermann, *Int. J. High Pressure Res.*, 1996, **14**, 235–248.
- 19 A. Boultif and D. Louer, *J. Appl. Crystallogr.*, 2004, **37**, 724–731.
- 20 V. Favre-Nicolin and R. Černý, *J. Appl. Crystallogr.*, 2002, **35**, 734–743.
- 21 A. A. Coelho, TOPAS-Academic; <http://members.optusnet.com.au/~alancoelho>.
- 22 A. L. Spek, *PLATON*. University of Utrecht, The Netherlands, 2006.
- 23 B. Efron and R. Tibshirani, *Stat. Sci.*, 1986, **1**, 54–77.
- 24 R. Domènec-Ferrer, F. Ziegs, S. Klod, I. Lindemann, R. Voigtländer, L. Dunsch and O. Gutfleisch, *Anal. Chem.*, 2011, **83**, 3199–3204.
- 25 B. Krebs, H. Greiving, C. Brendel, F. Taulelle, M. Gaune-Escard and R. W. Berg, *Inorg. Chem.*, 1991, **30**, 981–988.
- 26 G. Mairesse, P. Barbier and J. P. Wignacourt, *Acta Crystallogr., Sect. B: Struct. Crystallogr. Cryst. Chem.*, 1979, **35**, 1573–1580.
- 27 R. Černý, D. B. Ravnsbæk, G. Severa, Y. Filinchuk, V. D'Anna, H. Hagemann, D. Haase, C. M. Jensen and T. R. Jensen, *J. Phys. Chem. C*, 2010, **114**, 19540–19549.
- 28 S. Aldridge, A. J. Blake, A. J. Downs, R. O. Gould, S. Parsons and C. R. J. Pulham, *J. Chem. Soc., Dalton Trans.*, 1997, 1007–1012.
- 29 K. B. Harvey and N. R. McQuaker, *Can. J. Chem.*, 1971, **49**, 3282.
- 30 J. Hvilstendahl, P. Klaeboe, E. Ryter and H. A. Oye, *Inorg. Chem.*, 1984, **23**, 706–714.
- 31 B. C. Knutz, R. W. Berg, H. A. Hjuler and N. J. Bjerrum, *J. Electrochem. Soc.*, 1993, **140**, 3380–3390.
- 32 K. S. Mohandas, N. Sanil, T. Mathews and P. Rodriguez, *Metall. Mater. Trans. B*, 2001, **32**, 669–677.